Aerosol and Air Quality Research, 13: 1832–1846, 2013

ISSN: 1680-8584 print / 2071-1409 online
doi: 10.4209/aaqr.2012.10.0283

Spatial and Temporal Variation of Chemical Composition and Mass Closure of Ambient PM_{10} in Tianjin, China

Tianru Ni[1], Penghui Li[1], Bin Han[2], Zhipeng Bai[2*], Xiao Ding[1], Qianwen Wang[1], Jing Huo[1], Bing Lu[1]

[1] *College of Environmental Science and Engineering, Nankai University, Tianjin, 300071, China*
[2] *State Key Laboratory of Environmental Criteria and Risk Assessment, Chinese Research Academy of Environmental Sciences, Beijing, 100012, China*

ABSTRACT

A one-year monitoring program from September 2009 to August 2010 for PM_{10} was conducted at 8 monitoring sites in Tianjin, a coastal city in northern China. 24-hour PM_{10} samples were collected every 6 days at each site. PM_{10} samples were analyzed for elements, water soluble inorganic ions and carbonaceous species. This paper focused on the spatial and temporal variation of chemical composition and chemical mass closure of ambient PM_{10}. Six categories were used to reconstruct PM_{10} mass: crustal materials, trace elements, organic matter, elemental carbon, sea salt, and secondary inorganic aerosol. Crustal materials were the dominant fraction of PM_{10} with annual average percentages varying from 31.6% to 33.8% of the total PM_{10} mass. Secondary inorganic aerosol (non-sea salt sulfate, nitrate and ammonium) and organic matter were also major contributors to PM_{10}, with annual mass fractions of 23.3% and 18.8%, respectively. In particular, non-sea salt-sulfate was the most predominant inorganic ion accounting for 47.9% of the category of secondary inorganic aerosol. Elemental carbon was a small category, accounting for 3.3%. Sea salt and trace elements contributed marginally to the PM_{10} mass. The concentrations and mass fractions of crustal materials were generally highest in spring and lowest in summer while those of organic matter and secondary inorganic aerosol were generally highest in winter. Organic matter ($P < 0.05$) and elemental carbon ($P < 0.001$) concentrations showed significant spatial variations, and the concentrations were high at Beichen (BC) due to its proximity to the industrial zones and freeways. The concentrations of Ba, Zn, Pb, Sn, Sb were generally higher at BC and Hongqiao (HQ) than at other sites, suggesting higher influence of traffic emissions.

Keywords: Mass closure; Chemical composition; PM_{10}; Tianjin.

INTRODUCTION

Atmospheric particulate matter (PM) is a complex mixture of numerous compounds originating from a large variety of processes associated with both natural and anthropogenic sources. Recent epidemiological studies have shown a consistent association of the mass concentration of PM_{10} (particles of aerodynamic diameter smaller than 10 μm) with adverse effects on human health (Sanhueza *et al.*, 2009; Clark *et al.*, 2010; Ohlson *et al.*, 2010; Hart *et al.*, 2011). PM can also cause ambient air quality problems, such as visibility reduction (Watson, 2002). Furthermore, PM can affect the earth's radiation balance and consequently the climate, by scattering and absorbing solar and thermal infrared radiation and by serving as condensation nuclei for the cloud formation (IPCC, 2001). All these effects on radiation depend on the size, shape, and chemical composition of the particles (IPCC, 2001). Toxicological studies have attempted to identify which particle characteristics are responsible for which adverse biological responses (e.g., particle number, size, surface, chemical composition), and suggested that the chemical composition of PM plays an important role in these responses (Sandstrom *et al.*, 2005). The chemical composition of PM may vary largely depending on PM sources (because of a large number of sources in urban areas), and can reflect differences in source contributions. Thus, efforts have been made over years to elucidate the chemical composition of PM, and to achieve mass closure on the chemical species for the whole mass of PM collected (Matta *et al.*, 2003). The spatial and temporal variation of PM chemical composition greatly depends on factors such as emission/transformation rate, distance of sources, physical conditions of the medium where they are introduced (Perrino *et al.*, 2010; Singh *et al.*, 2012; Saitanis *et al.*, 2013) and meteorological conditions (e.g., mixing depth of the atmosphere, rainfall, wind speed and prevailing wind direction).

* Corresponding author. Tel.: +8601084915246
E-mail address: zbai@nankai.edu.cn

Concerns on the levels of PM_{10} have led to the establishment of daily and annual limit values for PM_{10} starting from 1996 in China (Ministry of Environmental Protection of the People's Republic of China, 1996) and the annual limit value was decreased from 100 μg/m^3 to 70 μg/m^3 in 2012 (Ministry of Environmental Protection of the People's Republic of China, 2012). Tianjin is an important coastal city with high PM_{10} concentration due to intensive energy consumption and large industrial activities. The chemical compositions of PM in this area are influenced by both natural and anthropogenic sources, such as wind and soil erosion, construction activities, sea salt, fossil-fuel combustion, industrial processes, vehicular emissions and photochemical reactions (Ho *et al.*, 2006; Tsai and Chen, 2006). However, available data for long-term monitoring, chemical composition and mass closure analysis of ambient PM_{10} were limited in Tianjin. In the present study, a one-year (from September 2009 to August 2010) monitoring program was conducted for the first time in Tianjin collecting 24 h PM_{10} samples every 6 days at 8 monitoring sites. The purpose of the study was (a) to determine the spatial and seasonal characteristics of PM_{10} chemical compositions including crustal materials (CM), trace elements (TE), organic matter (OM), elemental carbon (EC), sea salt (SS), and secondary inorganic aerosol (SIA); (b) to quantify the relative contribution of these compositions and to identify the major fractions of PM_{10} mass by using mass closure model; (c) to test whether the gravimetrically determined mass can be reconstructed by the chemically determined constituents.

METHODOLOGY

Sampling Sites Description

Tianjin is a coastal city located in the eastern part of northern China. It experiences a continental monsoonal climate, with characteristic of hot, humid summer, and dry, cold winter. The mean annual temperature and precipitation is 13.1°C and 389.4 mm, respectively and more than half of the annual rainfall occurs in summer (Table 1) (Du *et al.*, 2010, 2011). The domestic heating season is generally between November and March due to the cold weather.

Eight sites, Beichen (BC), Dongli (DL), Hebei (HB), Hedong (HD), Hongqiao (HQ), Hexi (HX), Shizhan (SZ) and Tieta (TT) were selected for PM_{10} monitoring (Table 2). The location of each site is shown in Fig. 1. DL and BC were chosen to represent suburban sites and the other six sites are located in the urban area. Several industrial zones are located in the suburban area of Tianjin, and the main industries are oil refining, petrochemical facilities, iron and steel manufacturing, non-ferrous metal smelting, cement production, transportation, food, electronic and biological pharmaceutics, etc. BC is near freeways with a large volume and high fraction of heavy duty diesel vehicles (HDDVs).

PM_{10} Sampling and Mass Measurement

The one-year sampling campaign was conducted from September 2009 to August 2010 at the 8 monitoring sites except for HD (December 2009 to August 2010). 24-hour PM_{10} samples were collected every 6 days at each site. Moreover, daily PM_{10} samples were collected during four periods from Oct. 22 to Oct. 28, Dec. 21 to Dec. 27, 2009, and Apr. 8 to Apr. 14, July 14 to July 19, 2010. At each site, two medium-volume samplers (Model TH-150S, manufactured by Tianhong Instrument Co., Ltd. Wuhan, China) operating at 100 L/min with a 10 μm cut-point impactor were used in parallel to collect PM_{10} samples on polypropylene filters (Ø = 90 mm, Beijing Synthetic Fiber Research Institute, China) for elemental analysis and determination of gravimetric values of PM_{10}, and on quartz

Table 1. Seasonal meteorological characteristics in Tianjin.

Season[a]	Average Temperature (°C)	Average relative humidity (%)	Total precipitation (mm)	Average wind speed (m/s)
Autumn	13.9	58.3	70.2	1.5
Winter	–1.4	48.0	18.0	1.6
Spring	12.9	47.3	59.1	2.0
Summer	26.9	65.3	242.1	1.2
Annual	13.1	56.9	389.4	1.6

[a] Autumn: 10/09/2009–27/11/2009; Winter: 03/12/2009–25/02/2010; Spring: 03/03/2010–26/05/2010; Summer: 01/06/2010–30/08/2010.

Table 2. Overview of the sampling sites.

Sites	Sites description	Height (m)	Number of samples
Beichen (BC)	Suburban, industrial site, near to freeway	10.0	71
Dongli (DL)	Suburban, industrial site	10.0	71
Hebei (HB)	City centre, near to construction site	10.0	66
Hedong (HD)	City centre, traffic, residential and commercial site	10.0	42
Hongqiao (HQ)	City centre, near to densely trafficked roads and construction site	18.0	70
Hexi (HX)	City centre, traffic, residential and commercial site	19.5	71
Shizhan (SZ)	City centre,traffic, residential and commercial site	21.0	72
Tieta (TT)	City centre,traffic, residential and commercial site	10.0	66

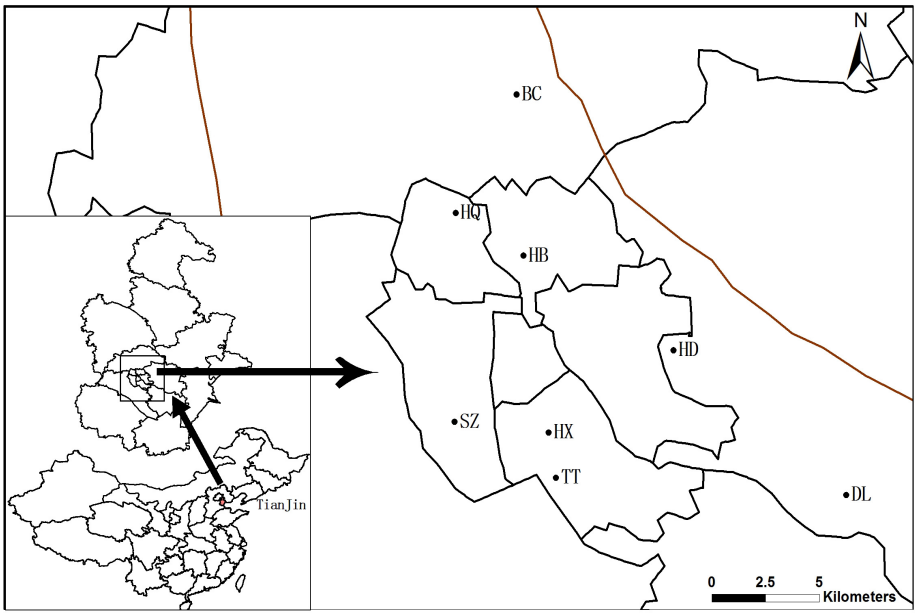

Fig. 1. Location of the eight sites.

fiber filters (Ø = 90 mm, Pall Gelman Laboratory, Ann Arbor, MI, USA) for ionic/carbonaceous species analysis.

Polypropylene filters and quartz fiber filters were pre-fired (polypropylene filters: 60°C for 0.5 h, quartz fiber filters: 800°C for 2 h) to remove any organic compounds that may be present on the filters, and then pre-conditioned at room temperature for 48h in a desiccator before sampling. After PM_{10} collection, the filters were reconditioned for another 48 h and subsequently analyzed for total mass. Filters were weighed before and after sampling by a microbalance (Meter Toledo M5) with balance sensitivity ± 0.010 mg. After re-weighing, the exposed filters were stored in a freezer at –4°C before chemical analysis to prevent the evaporation of volatile components.

Chemical Analyses

Half of each polypropylene filter was cut into portions and then digested to extract metals with a nitric acid solution. The extracted solution was filtered and then diluted with distilled/deionized water. The solution was then analyzed by different instruments. Si, Al, Mg, Ca, Fe, Ti, Ba and Sr were analyzed by inductively coupled plasma-optical emission spectrometry (Kong *et al.*, 2011b) (ICP-OES) (IRIS Intrepid II, Thermo Electron), and K, Na, P, V, Cr, Mn, Co, Ni, Cu, Zn, As, Rb, Y, Mo, Cd, Sn, Sb, La, Ce, Tl and Pb were analyzed by inductively coupled plasma-mass spectroscopy (Kong *et al.*, 2011b) (ICP-MS) (Agilent 7500a, Agilent Co. USA). The ICP-OES and ICP-MS were calibrated using a high-purity standard solution. More details about the extraction of elements, ICP-OES and ICP-MS analysis methods and calibration are available in previous studies (Kong *et al.*, 2010, 2011a, b). The method detection limits (MDLs) of an analysis was defined as the value of standard deviation in the replicate analysis of blanks, multiplied by a conservative factor of three (Chan *et al.*, 1999). The MDLs were 69 μg/L, 45 μg/L, 47 μg/L, 39 μg/L, 181 μg/L, 24 μg/L, 2 μg/L, 0.4 μg/L, 41 μg/L and 31 μg/L for Si, Al, Mg, Ca, Fe, Ti, Ba, Sr, K and Na respectively, 4.6 μg/L, 0.92 μg/L, 0.07 μg/L, 0.67 μg/L, 0.38 μg/L, 0.02 μg/L, 0.36 μg/L, 1.1 μg/L, 0.57 μg/L, 0.22 μg/L and 0.01 μg/L for Zn, P, V, Cr, Mn, Co, Ni, Cu, As, Rb and Y respectively, and 0.05 μg/L, 0.01 μg/L, 0.04 μg/L, 0.03 μg/L, 0.16 μg/L, 0.02 μg/L, 0.004 μg/L and 0.22 μg/L for Mo, Cd, Sn, Sb, La, Ce, Tl and Pb respectively.

In preparation for water soluble ions analysis (Na^+, NH_4^+, Mg^{2+}, K^+, Ca^{2+}, Cl^-, SO_4^{2-} NO_3^-), quarter sections of the quartz fiber filters were extracted by using 10 mL of ultra-pure water (specific resistance ≥ 18 MΩ cm). The extraction solutions were filtered, drawn into a syringe, and then injected into a Dionex DX-120 Ion Chromatograph (IC) (DX-120, Dionex Ltd., USA) with flow rate of 1.0 mL/min which consisted of columns for cations (CS12A) and anions (AS11-HC) (Kong *et al.*, 2011a). The MDLs were 0.0125 mmol/L, 0.0020 mmol/L, 0.0026 mmol/L, 0.0032 mmol/L and 0.0050 mmol/L for Na^+, NH_4^+, Mg^{2+}, K^+ and Ca^{2+} respectively and 0.0072 mmol/L, 0.0696 mmol/L and 0.0385 mmol/L for Cl^-, SO_4^{2-} and NO_3^- respectively.

Another quarter of each quartz fiber filter was used for analysis of organic carbon (OC) and elemental carbon (EC) by improve thermal/optical reflectance (TOR) method with DRI Model 2001 Thermal/Optical Carbon Analyzer (Louie *et al.*, 2005). The MDLs for OC and EC was 0.82 μg C/cm^2 and 0.19 μg C/cm^2.

Quality Assurance

Each filter was weighed 3 times before and after sampling and the average value was used. Blanks (including filters) and duplicate sample analyses were performed for approximately 10% of all the samples (Ni *et al.*, 2012). Blank filters were processed simultaneously with field samples. Sample spike recoveries were in the range of 80–120%. For elemental analysis, geochemistry reference matter

including GBW07402 (GSS-2) and GBW07406 (GSS-6)) from the Center for National Standard Matter were simultaneously analyzed to check the precision of analysis. Precision of ICP-OES analysis ranged between 2.79% and 5.50% while precision of ICP-MS analysis were in the range of 2.04–14.65% with most being < 7% for individual elements. For water soluble ions analysis, standard solutions were prepared and were detected for three times, and the precision ranged between 0.46% and 3.00%. For OC and EC analysis, standard concentrations of CH_4/CO_2 mixed gases were used for calibration of the analyzer before and after sample analysis. The analysis precision was less than 2%.

PM_{10} Mass Balance Closure

For the purpose of chemical mass closure, the chemical components were divided into six categories as follows: crustal materials (CM), trace elements (TE), organic matter (OM), elemental carbon (EC), sea salt (SS), and secondary inorganic aerosol (SIA). CM represents the sum of typical crustal materials, including Al, Si, Mg, K, Ca, Fe and Ti. Each of these species was multiplied by an appropriate factor to account for its common oxides based on the following equation (Marcazzan *et al.*, 2001; Hueglin *et al.*, 2005; Cheung *et al*., 2011).

$$CM = 1.89Al + 2.14Si + 1.66Mg + 1.21K + 1.40Ca + 1.43Fe + 1.67Ti \quad (1)$$

TE included elements such as Ba, Sr, Na, P, V, Cr, Mn, Co, Ni, Cu, Zn, As, Rb, Y, Mo, Cd, Sn, Sb, La, Ce, Tl and Pb. OM was obtained by multiplying the measured concentration of organic carbon (OC) by a factor of 1.6 as proposed by Turpin and Lim (2001) for urban aerosol and used by several previous studies (Viana *et al.*, 2007; Vecchi *et al.*, 2008; Mkoma *et al.*, 2009; Terzi *et al.*, 2010). In this study, the SS contribution was calculated, assuming that soluble Na^+ in PM_{10} samples comes solely from sea salt, as the sum of Na^+ concentration and fractions of the concentrations of Cl^-, Mg^{2+}, K^+, Ca^{2+}, and SO_4^{2-} based on the standard sea water composition and ignoring atmospheric transformations (Seinfeld and Pandis, 2006):

$$SS = [Na^+] + [ss\text{-}Cl^-] + [ss\text{-}Mg^{2+}] + [ss\text{-}K^+] + [ss\text{-}Ca^{2+}] + [ss\text{-}SO4^{2-}] \quad (2)$$

where $[ss\text{-}Cl^-] = 1.8\,[Na^+]$, $[ss\text{-}Mg^{2+}] = 0.12\,[Na^+]$, $[ss\text{-}K^+] = 0.036\,[Na^+]$, $[ss\text{-}Ca^{2+}] = 0.038\,[Na^+]$, and $[ss\text{-}SO4^{2-}] = 0.252\,[Na^+]$ (Terzi *et al.*, 2010). The EC contribution was reported as determined by thermal desorption. The SIA contribution was calculated as the sum of non-sea salt (nss) SO_4^{2-}, NO_3^- and NH_4^+, where nss-SO_4^{2-} was calculated by subtracting ss-SO_4^{2-} from total SO_4^{2-} (Viana *et al.*, 2007; Terzi *et al.*, 2010).

RESULTS AND DISCUSSION

PM_{10} Concentrations

A total of 529 samples of PM_{10} were collected in this study. Statistical summaries of annual mass concentrations of selected chemical species and gravimetric PM_{10} at the 8 sampling sites are listed in Table 3, including the average concentrations and associated standard deviation. The average PM_{10} concentrations at these 8 sites ranged from 199.3 μg/m^3 to 233.6 μg/m^3 (Table 3) all exceeding the National Ambient Air Quality Standard (NAAQS) of 100 μg/m^3 (GB3095-1996, China), indicating the necessity for local authorities to implement appropriate measures for PM emissions reduction. Among the 8 sites, the average concentrations of PM_{10} at HQ (233.6 μg/m^3), HB (232.0 μg/m^3) and BC (228.4 μg/m^3) were higher than other sites, reflecting higher emissions at these three sites (probably from the construction activities carried out all around in the study period (HQ and HB), the nearby densely trafficked roads (HQ and BC), the nearby industrial area (BC)). In general, PM_{10} concentrations in Tianjin were higher than those in other Chinese cities such as Beijing (Zhang *et al.*, 2009; Wu *et al.*, 2011), Shanghai (Li *et al.*, 2012) and Guangzhou (Yu *et al.*, 2012). Although not shown in the table, higher overall PM_{10} mass concentrations were observed in winter (253.8 ± 29.3 μg/m^3) compared with spring (207.9 ± 6.8 μg/m^3), summer (185.8 ± 12.2 μg/m^3) and autumn (233.3 ± 20.5 μg/m^3). This is consistent with the results of Lazaridis *et al.* (2002), Matta *et al.* (2003) and Bi *et al.* (2007), which determined that increased coal combustion for domestic heating and frequent thermal inversions during winter lead to the higher PM_{10} level.

PM_{10} Mass Chemical Composition

Annual mean mass closures for PM_{10} at all measurement sites, computed as the averages of all daily mass concentrations, are listed in Table 4 to demonstrate the overall spatial variation of PM_{10} mass composition. The seasonal results of the chemical mass closure for PM_{10} are shown as mass concentrations and relative contributions in Fig. 2 and Fig. 3, respectively. The relative contributions are independent of dilution and reflect differences in emission sources and processes (e.g., transformation, rain) controlling the aerosol composition (Putaud *et al.*, 2004; Sillanpaa *et al.*, 2006). Crustal materials, organic matter, and secondary inorganic aerosol were the main contributors to PM_{10} mass concentrations at all sites. The spatial and temporal characteristics of the major contributors are discussed in detail in the following sections.

Crustal Materials and Trace Elements

Crustal materials originate from soil, and fugitive dust (Ho *et al.*, 2006). Table 4 shows that crustal materials dominated the PM_{10} profiles at all sites with average percentage of 31.6–33.8% of the total PM_{10} mass. The concentrations and mass fractions of crustal materials were generally highest in spring (Fig. 2 and Fig. 3) due to the high dust re-suspension and soil aridity, the influence of high wind speeds and the low precipitation in this season as shown in Table 1. The lowest concentrations and mass fractions of crustal materials were found in summer due to the little exposed land, and high soil moisture influence of abundant precipitation. Even though spatial variation of

Table 3. Statistical summary of annual mass concentrations (mean ± standard deviation) of selected chemical species and gravimetric PM_{10}.

Component	unit	SZ	TT	HX	HD	HB	HQ	DL	BC
PM_{10}	μg/m^3	199.3 ± 113.9	201.1 ± 82.8	206.2 ± 103.5	216.7 ± 93.7	232.0 ± 128.8	233.6 ± 139.5	212.4 ± 95.7	228.4 ± 110.9
SO_4^{2-}	μg/m^3	21.1 ± 20.0	25.2 ± 27.1	26.3 ± 24.7	25.5 ± 22.3	26.7 ± 24.6	27.1 ± 24.5	21.8 ± 13.9	27.9 ± 24.5
NO_3^-	μg/m^3	15.0 ± 9.9	15.2 ± 13.8	16.1 ± 14.6	16.1 ± 12.5	20.5 ± 20.8	22.1 ± 21.1	15.1 ± 10.9	18.6 ± 12.8
NH_4^+	μg/m^3	8.81 ± 4.87	9.85 ± 5.73	10.2 ± 7.91	9.47 ± 5.90	10.7 ± 8.57	9.02 ± 6.94	8.78 ± 6.85	10.5 ± 8.1
Na^+	μg/m^3	1.87 ± 1.09	1.71 ± 1.09	1.60 ± 0.80	1.64 ± 1.11	1.33 ± 0.95	1.50 ± 1.25	1.24 ± 1.03	1.58 ± 0.71
OC	μg/m^3	20.6 ± 15.2	22.7 ± 19.9	19.1 ± 10.3	22.2 ± 11.9	26.8 ± 24.8	28.5 ± 21.7	26.6 ± 19.6	27.9 ± 19.7
EC	μg/m^3	7.09 ± 4.90	8.05 ± 7.83	4.74 ± 1.47	6.94 ± 4.34	4.82 ± 3.60	5.15 ± 2.33	5.64 ± 2.92	10.6 ± 13.3
Si	μg/m^3	13.5 ± 10.1	14.1 ± 9.9	12.9 ± 8.4	15.6 ± 11.7	16.3 ± 11.5	17.7 ± 15.7	14.8 ± 10.3	15.7 ± 11.1
Al	μg/m^3	5.96 ± 3.82	6.01 ± 4.08	5.42 ± 3.41	6.30 ± 4.24	6.68 ± 4.45	6.93 ± 5.10	6.17 ± 4.07	6.66 ± 4.14
Mg	μg/m^3	1.83 ± 1.28	1.96 ± 1.40	1.77 ± 1.22	1.95 ± 1.19	2.23 ± 1.63	2.47 ± 1.97	2.06 ± 1.28	2.41 ± 1.47
K	μg/m^3	2.80 ± 2.21	2.97 ± 1.99	2.80 ± 1.95	3.00 ± 1.69	3.08 ± 2.48	3.38 ± 2.85	3.18 ± 2.16	3.09 ± 2.38
Ca	μg/m^3	6.65 ± 4.21	7.86 ± 5.98	6.69 ± 4.17	6.96 ± 3.36	8.67 ± 5.68	9.48 ± 6.42	8.00 ± 4.68	9.36 ± 5.88
Fe	μg/m^3	4.32 ± 3.46	4.73 ± 3.31	4.64 ± 3.10	4.80 ± 3.07	5.16 ± 3.95	5.58 ± 4.11	5.40 ± 3.45	5.13 ± 3.71
Na	μg/m^3	1.80 ± 1.07	1.90 ± 1.07	1.70 ± 1.00	2.02 ± 1.59	1.83 ± 1.11	2.08 ± 1.40	1.84 ± 1.01	1.93 ± 1.13
Zn	μg/m^3	1.01 ± 9.57	1.20 ± 0.99	1.11 ± 0.94	1.02 ± 0.76	1.13 ± 0.99	1.20 ± 0.99	1.07 ± 0.98	1.35 ± 1.34
Ti	ng/m^3	332 ± 234	416 ± 650	294 ± 195	349 ± 243	360 ± 265	382 ± 293	358 ± 251	399 ± 266
Ba	ng/m^3	97.7 ± 81.1	91.4 ± 71.9	82.7 ± 65.4	86.6 ± 60.9	93.6 ± 75.6	110 ± 94.9	101 ± 75.8	108 ± 84.7
Sr	ng/m^3	42.8 ± 29.9	40.4 ± 27.2	38.8 ± 25.6	41.5 ± 25.6	42.9 ± 30.0	49.1 ± 33.6	38.7 ± 24.0	46.4 ± 30.9
P	ng/m^3	150 ± 100	157 ± 98.5	166 ± 129	188 ± 140	182 ± 111	185 ± 119	195 ± 171	177 ± 121
V	ng/m^3	10.9 ± 8.67	11.9 ± 9.77	11.3 ± 7.33	12.9 ± 7.82	12.9 ± 9.27	13.5 ± 11.3	18.1 ± 22.2	12.6 ± 10.3
Cr	ng/m^3	21.3 ± 20.9	23.9 ± 42.6	15.9 ± 8.26	21.2 ± 12.1	19.6 ± 11.5	32.1 ± 98.6	20.1 ± 8.90	37.5 ± 59.7
Mn	ng/m^3	407 ± 853	349 ± 1006	184 ± 131	186 ± 107	196 ± 149	194 ± 149	210 ± 184	556 ± 1206
Co	ng/m^3	2.34 ± 1.06	2.28 ± 1.27	2.17 ± 1.43	2.40 ± 1.27	2.68 ± 1.92	3.10 ± 2.44	2.18 ± 1.32	2.82 ± 1.89
Ni	ng/m^3	10.0 ± 6.07	13.0 ± 22.1	9.22 ± 5.19	10.2 ± 4.54	11.5 ± 7.83	12.3 ± 7.95	10.5 ± 5.45	15.6 ± 24.7
Cu	ng/m^3	211 ± 314	190 ± 381	92.1 ± 114	245 ± 185	140 ± 140	149 ± 159	81.8 ± 96.7	225 ± 342
As	ng/m^3	18.5 ± 27.4	20.9 ± 41.9	21.1 ± 33.6	18.6 ± 23.8	22.0 ± 37.3	23.4 ± 32.1	17.3 ± 33.8	22.8 ± 34.2
Rb	ng/m^3	13.7 ± 12.6	13.4 ± 10.4	13.4 ± 10.3	13.3 ± 8.43	14.6 ± 13.2	16.4 ± 16.9	14.9 ± 11.5	15.1 ± 13.3
Y	ng/m^3	2.71 ± 1.90	2.80 ± 1.82	2.66 ± 1.59	3.09 ± 1.84	3.16 ± 2.20	3.42 ± 2.66	2.91 ± 1.96	3.21 ± 2.28
Mo	ng/m^3	2.15 ± 1.85	2.44 ± 2.57	2.29 ± 1.79	2.30 ± 1.63	2.29 ± 1.85	2.63 ± 2.34	4.22 ± 7.77	2.78 ± 2.00
Cd	ng/m^3	5.04 ± 4.93	4.82 ± 4.00	4.90 ± 4.74	4.61 ± 4.28	5.35 ± 5.09	5.71 ± 5.49	4.45 ± 4.00	5.62 ± 4.86
Sn	ng/m^3	14.1 ± 14.8	15.3 ± 17.6	14.2 ± 16.6	15.1 ± 15.6	17.0 ± 19.4	23.5 ± 43.8	10.4 ± 11.2	22.0 ± 20.0
Sb	ng/m^3	12.4 ± 14.7	15.7 ± 28.2	11.0 ± 18.6	9.2 ± 11.3	13.1 ± 16.9	16.3 ± 26.9	10.0 ± 13.6	17.8 ± 22.5
La	ng/m^3	7.01 ± 7.30	6.20 ± 4.79	6.00 ± 4.61	6.27 ± 3.87	7.86 ± 7.63	8.10 ± 6.78	5.61 ± 3.70	7.77 ± 7.12
Ce	ng/m^3	8.15 ± 6.55	8.22 ± 5.82	7.71 ± 5.43	8.65 ± 5.64	9.61 ± 7.56	9.92 ± 7.62	8.37 ± 6.28	9.20 ± 6.81
Tl	ng/m^3	2.09 ± 1.75	2.07 ± 1.70	2.11 ± 1.73	1.81 ± 1.27	2.06 ± 1.68	2.25 ± 1.90	1.85 ± 1.56	2.01 ± 1.61
Pb	ng/m^3	220 ± 194	252 ± 191	247 ± 193	232 ± 151	272 ± 249	309 ± 398	227 ± 154	305 ± 269

Table 4. Annual mass concentrations and relative contributions (%) of PM_{10} components[a].

Component	SZ $\mu g/m^3$ (%)	TT $\mu g/m^3$ (%)	HX $\mu g/m^3$ (%)	HD $\mu g/m^3$ (%)	HB $\mu g/m^3$ (%)	HQ $\mu g/m^3$ (%)	DL $\mu g/m^3$ (%)	BC $\mu g/m^3$ (%)
CM	62.6 (32.5)	66.8 (33.8)	56.6 (31.6)	69.4 (32.5)	74.7 (33.6)	76.8 (33.3)	70.3 (33.7)	73.7 (31.9)
TE	3.9 (2.0)	4.2 (2.1)	3.6 (1.7)	4.0 (1.8)	3.8 (1.8)	4.3 (1.9)	3.7 (1.8)	4.7 (2.2)
OM	33.0 (18.7)	36.3 (18.8)	30.6 (15.8)	35.6 (18.2)	42.8 (18.9)	45.6 (20.2)	42.5 (19.4)	44.6 (20.1)
EC	7.1 (4.0)	8.1 (3.9)	4.7 (2.4)	6.9 (3.5)	4.8 (2.5)	5.2 (2.8)	5.6 (2.8)	10.6 (4.7)
SIA	44.4 (22.0)	49.8 (24.1)	52.1 (24.3)	50.6 (23.1)	57.5 (23.8)	57.8 (23.9)	45.2 (21.1)	56.5 (24.1)
SS	6.1 (3.1)	5.6 (2.8)	5.1 (2.6)	5.3 (2.4)	4.3 (1.9)	4.9 (2.3)	4.6 (2.2)	5.1 (2.4)
Unidentified	41.1 (16.4)	27.2 (14.4)	50.4(17.9)	40.4 (18.1)	43.2 (17.4)	29.8 (14.9)	42.9 (18.6)	32.0 (12.1)

[a] CM: crustal materials; TE: trace elements; OM: organic matter; EC: elemental carbon; SIA: secondary inorganic aerosol ; SS: sea salt.

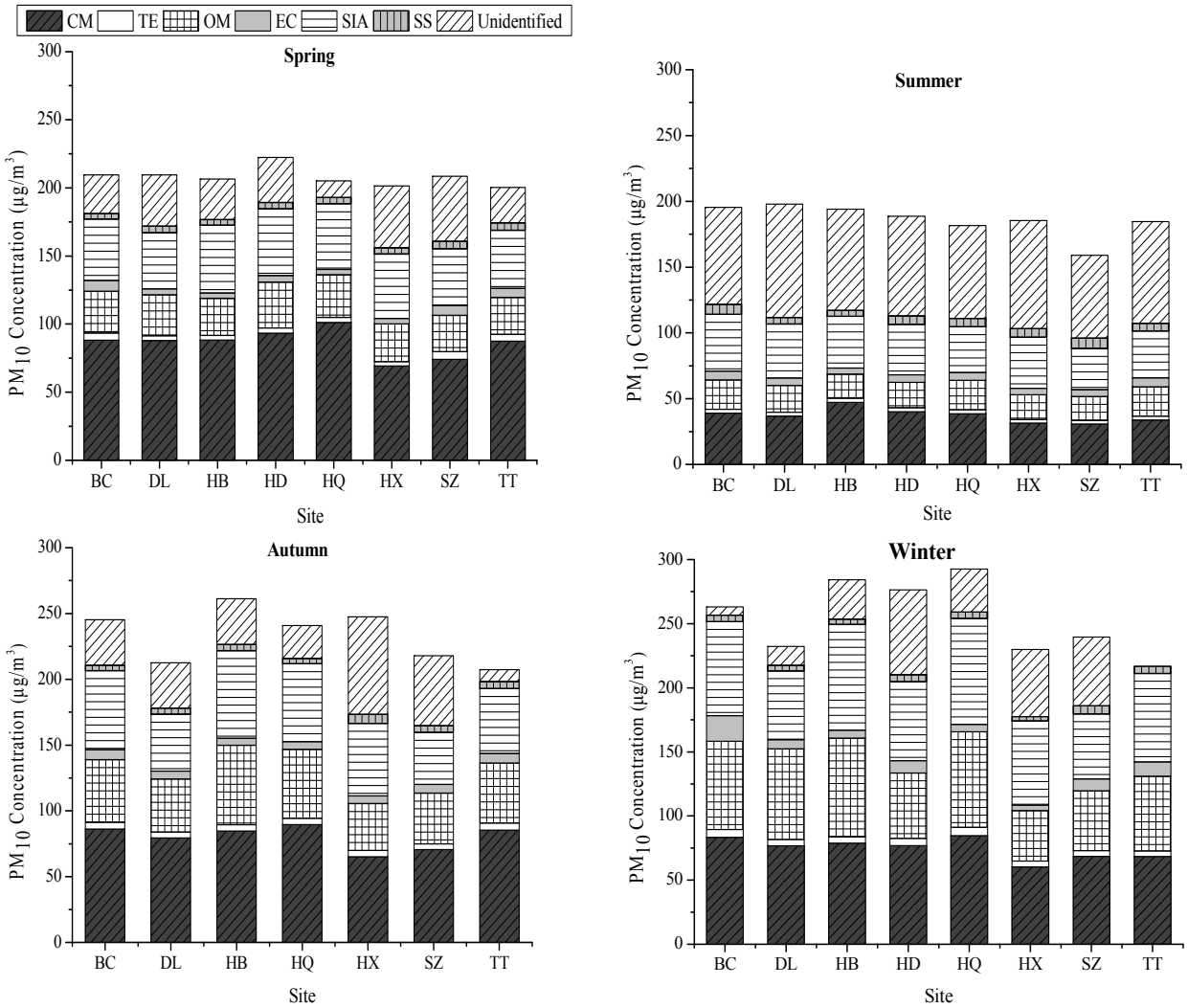

Fig. 2. The mass concentrations of chemical components and unidentified matter of PM_{10}. CM: crustal materials; TE: trace elements; OM: organic matter; EC: elemental carbon; SIA: secondary inorganic aerosol; SS: sea salt.

crustal materials concentrations at the 8 sites was not significant ($P > 0.05$), elevated concentrations were found at HQ for all seasons except for summer (Fig. 2). The elevated crustal materials concentrations at HQ may be attributed to traffic-induced re-suspension of road dust and emissions from construction sites. The contributions of crustal materials in this study were much higher than those reported for cities in Switzerland (10.0%–15.0%) (Hueglin *et al.*, 2005). High contributions of crustal materials were also observed in Athens (Sillanpaa *et al.*, 2006), Barcelona (Viana *et al.*, 2007) and Los Angeles (Cheung *et al.*, 2011). It has been reported that crustal materials contributions are generally high in northern China due to the exposed lands and dust re-suspension (Sun *et al.*, 2011).

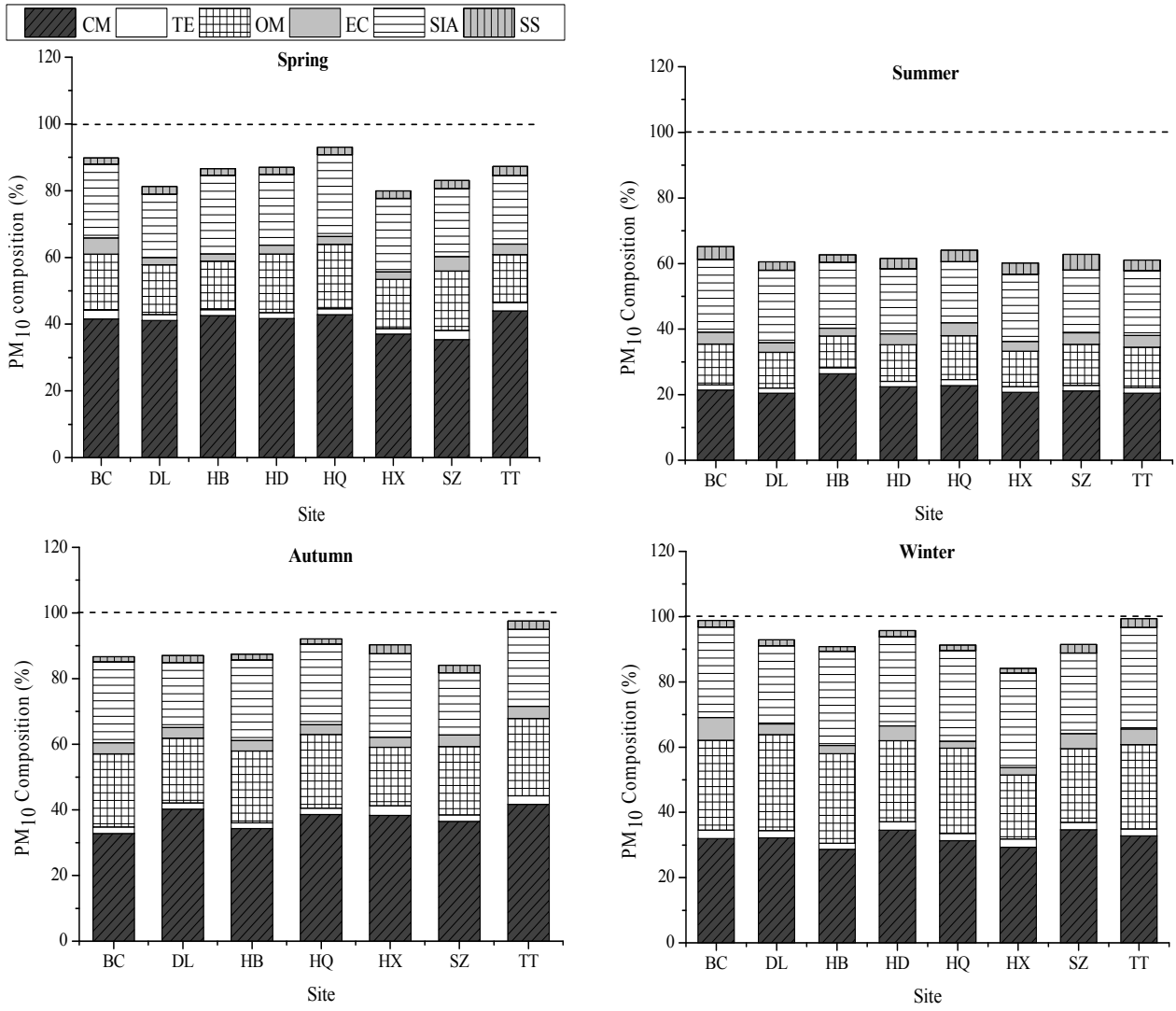

Fig. 3. The relative contributions of chemical components to PM_{10}. Dotted lines represent 100%. CM: crustal materials; TE: trace elements; OM: organic matter; EC: elemental carbon; SIA: secondary inorganic aerosol; SS: sea salt.

In this study, Si and Ca were the two most abundant mineral species, together with Al, their sum accounted for an average of 73.7% of total measured crustal elements. Among the 8 sites, HQ exhibited the highest annual Si, Ca, Al, Fe, K, and Mg concentrations while the highest annual Ti concentration was found at TT (Table 3). Moreover, higher Ca concentration at BC than at other sites (except for HQ) was also found attributed to emissions from cement production in the vicinity of BC site.

The trace elements were minor components of the PM_{10} at all sites, with annual mean contributions of about 2% (Table 4). The absolute concentration of the various trace elements was highly differentiated, ranging from 1.81 ± 1.27 ng/m^3 up to 2.08 ± 1.40 μg/m^3 (Table 3). Most elements (Ba, Sr, Na, P, V, Cr, Mn, Co, Ni, Cu, As, Rb, Y, Cd, Sb, La, Ce and Pb) exhibited the lowest concentrations in summer (data not shown in the table) due to the lack of some sources (typically related to house heating) and to a better dispersion of pollutants in the atmosphere. The concentrations of Ba, Zn, Pb, Sn and Sb were generally higher at BC and HQ than at other sites, suggesting higher influence of traffic emissions (Hueglin *et al.*, 2005; Hjortenkrans *et al.*, 2007; Terzi *et al.*, 2010). As discussed earlier, HQ is located near densely trafficked roads while BC is located near freeways with a large volume and high fraction of heavy duty diesel vehicles (HDDVs). HDDVs are known to induce larger amount of dusts emissions than light duty vehicles due to higher particle res-suspension and stronger abrasion processes (including tire wear and brake linings) (Charron and Harrison, 2005). For Ni, Cr and Mn, they showed the highest annual average values at BC reflecting the influence of industrial emissions such as metallurgical processes.

In order to assess the extent of the contribution of anthropogenic emissions to atmospheric elemental levels, the enrichment factors (EFs) were calculated by dividing the element abundance in the PM_{10} sample by their average abundance in Tianjin soil (China National Environmental Monitoring Centre, 1990):

$$EFs = (X/Al)_{PM10}/(X/Al)_{soil}. \quad (3)$$

Al was selected as reference element. The EFs for elements in PM_{10} samples are presented in Table 5. Generally, most elements showed similar EFs among the 8 sites. For Mg, K, Fe, Ti, Na, V, Rb, Y, La, Ce Ca, Ba, Sr, Cr, Mn, Co, Ni and Mo, the EFs were smaller than 10, indicating that these elements were non-enriched and mostly derived from crustal source (Chester *et al.*, 2000; Tecer *et al.*, 2012); while for Cu, As, Sn and Tl, the EFs were in the range of 10 to 100, suggesting that both natural emissions and anthropogenic sources were important for these elements; For those elements with average EFs larger than 100 including Zn, Cd, Sb and Pb, must have been affected significantly by anthropogenic sources (Kim *et al.*, 2004; Gugamsetty *et al.*, 2012). The high EFs for Cu, Zn, As, Cd, Sn, Sb, Tl and Pb can be attributed to emissions from metal industry, coal combustion and abrasion of brakes and clutch, etc. in automotive vehicles (Hueglin *et al.*, 2005; Sillanpaa *et al.*, 2006). In this study, Zn, Cd, Sb and Pb exhibited high EFs (EFs > 100), and the high EFs for these elements were also found by other authors at Chinese sites (Wei *et al.*, 1999; Wang *et al.*, 2006a; Han *et al.*, 2010).

Carbonaceous Compounds

The organic matter and EC had significant (18.8 ± 1.4%) and moderate (3.3 ± 0.8%) contributions to PM_{10} (Table 4), respectively. The concentrations and relative contributions of organic matter in PM_{10} showed a trend of winter > autumn > spring > summer at all sites as shown in Fig. 2 and Fig. 3. EC concentrations were generally higher in winter than those in other seasons at all sites except for HQ and HX. EC is a product of incomplete combustion from residential coal, motor vehicle fuel, and biomass while OC originates from primary anthropogenic sources like above combustions and from formation by chemical reactions in the atmosphere (Cao *et al.*, 2007). The higher OC and EC concentrations in winter can be attributed to increasing coal combustion for domestic heating and more frequent temperature inversions in this season while the lower OC and EC concentrations in summer may be due to the increased mixing depth and more rainy days causing the particulate matters to be washed out in the atmosphere in this season (Ho *et al.*, 2006). Similar seasonal variation of OC and EC concentrations (higher in winter and lower in summer) have been also reported in Hong Kong (Ho *et al.*, 2006) and Thessaloniki (Terzi *et al.*, 2010). There were significant diversities for organic matter ($P < 0.05$) and EC ($P < 0.001$) concentrations among the 8 sites. Levels of organic matter were higher at DL, BC, HB and HQ compared with other four sites (Table 4), especially during winter (Fig. 2). The higher organic matter levels at DL and BC were mainly due to their proximity to the industrial zones with coal as the predominant fuels. In the industrial zones,

Table 5. Enrichment factors of individual elements. The reference element is Al.

metals	B[a] (mg/kg)	SZ	TT	HX	HD	HB	HQ	DL	BC
Mg	12700	1.77	1.88	1.88	1.79	1.93	2.05	1.92	2.08
Al	73200	1.00	1.00	1.00	1.00	1.00	1.00	1.00	1.00
K	22000	1.56	1.64	1.72	1.59	1.54	1.63	1.71	1.54
Ca	23400	3.49	4.09	3.86	3.46	4.06	4.28	4.05	4.40
Fe	34100	1.56	1.69	1.84	1.64	1.66	1.73	1.88	1.65
Ti	3600	1.13	1.41	1.11	1.13	1.10	1.12	1.18	1.22
Na	14500	1.52	1.59	1.59	1.62	1.38	1.51	1.50	1.46
Ba	520	2.31	2.14	2.15	1.94	1.97	2.24	2.30	2.29
Sr	200	2.63	2.46	2.62	2.41	2.35	2.59	2.30	2.55
V	85.2	1.57	1.70	1.79	1.76	1.66	1.67	2.52	1.63
Cr	84.2	3.10	3.45	2.54	2.93	2.55	4.03	2.83	4.89
Mn	686	7.30	6.20	3.62	3.15	3.13	2.99	3.63	8.91
Co	13.6	2.12	2.04	2.16	2.05	2.16	2.41	1.90	2.28
Ni	33.3	3.68	4.77	3.74	3.58	3.79	3.91	3.74	5.14
Cu	28.8	89.94	80.49	43.21	98.87	53.24	54.67	33.69	85.75
Zn	79.3	156.12	184.86	188.36	149.94	155.75	160.41	159.21	186.59
As	9.6	23.69	26.50	29.74	22.54	25.17	25.71	21.34	26.08
Rb	112	1.50	1.46	1.62	1.38	1.43	1.55	1.57	1.48
Y	25.6	1.30	1.33	1.40	1.40	1.35	1.41	1.35	1.38
Mo	4.6	5.74	6.47	6.74	5.80	5.47	6.04	9.87	6.64
Cd	0.09	688.19	652.19	735.32	595.50	651.82	671.04	586.69	686.39
Sn	2.7	64.35	69.07	71.06	64.87	69.15	92.14	45.74	89.42
Sb	1.21	125.57	158.42	122.88	87.94	119.08	142.37	97.61	161.59
La	47.5	1.81	1.59	1.71	1.53	1.81	1.80	1.40	1.80
Ce	75.3	1.33	1.33	1.38	1.34	1.40	1.39	1.32	1.34
Tl	0.569	45.11	44.26	50.16	36.96	39.59	41.79	38.54	38.81
Pb	21	128.80	146.23	158.71	128.45	141.98	155.66	127.89	159.52

[a] B indicates the background values for each metal in Chinese soil obtained from China National Environmental Monitoring Centre (1990).

abundant coal was consumed to provide energy for industrial production and large amount of pollutants including OC were released to atmosphere. Moreover, the wind is blowing from northwest direction for most of the year in Tianjin, and HB and HQ are located in the downwind of the industrial zones, which lead to the relatively higher organic matter levels at these two sites. EC concentration at BC was considerably higher than values at other sites especially in winter (Fig. 2) probably due to its location near freeways with higher number and proportion of HDDVs, which generally emit higher EC compared with light duty gasoline vehicles (Kleeman *et al.*, 2008; Oanh *et al.*, 2010).

Organic matter concentrations in this study (30.6–45.6 μg/m^3) were higher than those reported for Bern, Zurich and Basel (4.7–9.0 μg/m^3) while the organic matter contribution ratios were comparable to those of the three cities. On the contrary, EC concentrations in this study were comparable to those found in Bern, Zurich and Basel while the EC contribution ratios (2.4–4.7%) were lower when compared with the three cities (7.4–17.9%) (Hueglin *et al.*, 2005). In addition, contributions of organic matter and EC obtained in Tianjin were similar to those reported for Thessaloniki (Terzi *et al.*, 2010) and Flanders (Vercauteren *et al.*, 2011).

For this study, average OC/EC ratios were 4.8, 4.3, 3.7 and 2.3 in winter, autumn, spring and summer, respectively showing a clear prevalence of organic carbonaceous species over EC. The higher wintertime OC/EC ratio corresponded to increased coal combustion for heating. The OC/EC ratios in Tianjin were comparable to those previously found in the city (Gu *et al.*, 2010) as well as to those reported for other Chinese cities such as Guangzhou (Wang *et al.*, 2006a) and Xi'an (Cao *et al.*, 2005).

Secondary Inorganic Aerosol

Overall, secondary inorganic aerosol (SIA) contributed on average 23.3 ± 1.2% of the PM_{10} mass, with sulfate being the major component. Concentrations and mass fractions of SIA were higher in winter (67.4 ± 12.0 μg/m^3, 27.6 ± 2.3%) than in spring (45.7 ± 3.4 μg/m^3, 21.7 ± 1.8%), summer (37.8 ± 3.8 μg/m^3, 20.3 ± 1.3%) and autumn (53.3 ± 9.7 μg/m^3, 23.1 ± 2.6%) (Fig. 2 and Fig. 3). Although concentrations of SIA did not show significant ($P > 0.05$) spatial variation, they were slightly higher at HQ, HB and BC compared with other five sites (Table 4).

The seasonal variations of ions are mainly due to meteorological factors, such as temperature, relative humidity and wind speed, either favoring or adversely affecting the dispersion of pollutants in the atmosphere. Moreover, changes in source emission strength with time can also lead to these variations (Sun *et al.*, 2004). Fig. 4 shows the seasonal variations of ammonium, nss-sulfate and nitrate ions.

The dominant pathway for sulfate formation is the gas-to-particle conversion of sulfur-containing precursors such as SO_2, H_2S, CS_2, carbonyl sulfide (COS), dimethyl sulfide (DMS) to sulfate, in the presence of oxidizing species (e.g., H_2O_2) (Xiu *et al.*, 2004; Kumar and Sarin, 2010). Among the sulfur-containing compounds, sulfur dioxide is the largest contributor (Khoder, 2002; Kumar and Sarin, 2010), mainly from local industrial emissions (Wang *et al.*, 2006b) and coal combustion for domestic heating (Sun *et al.*, 2004). In addition, sulfate in ambient air can be also derived from sea-salt and regional soils (Kumar and Sarin, 2010). Sulfate particles of sea salt origins contributed to only 3.7% of total measured sulfate in this study. Therefore, sulfate was mainly from local combustion, likely to be coal combustion for industry and domestic heating in Tianjin. Nss-sulfate was the most abundant inorganic ion of PM_{10}, accounting for about 47.9% of the category of SIA, and 11.5% of total PM_{10} mass. On average, nss-sulfate concentration in winter was 1.3, 1.8 and 2.3 times those observed in autumn, spring and summer, respectively. It is believed that the industrial emissions would remain relatively constant throughout the year. Thus, the higher concentration of sulfate in winter was attributed to the increased consumption of coal for heating purpose which would emit abundant sulfur dioxide leading to the higher sulfate aerosol in this season (Sun *et al.*, 2004). Moreover, the cold weather during wintertime in Tianjin (Table 1) would accelerate the accumulation of sulfate due to poor dispersion (thermal inversions).

Nitrogen oxides, the most significant precursor of nitrate, can be converted into nitric acid in the atmosphere, which combines with NH_3 to form nitrate particles through homogeneous or heterogeneous photochemical reactions (Khoder, 2002; Xiu *et al.*, 2004). Nitrogen oxides are mainly from coal combustion and the traffic emissions in China (Sun *et al.*, 2004; Zhang *et al.*, 2007; Wang *et al.*, 2012). Nitrate concentrations in winter were higher than those in spring, summer and autumn as shown in Fig. 4. There were three reasons accounting for this: (1) coal combustion for heating during this season may evidently increase the nitrogen oxides emission, which would in turn form the nitrate as a secondary particle; (2) the low temperature in winter would favor gas-to-particle conversion of nitrogen oxides gas (Stelson and Seinfeld, 1982) and frequent thermal inversions in this cold season cause nitrate to accumulate in the lower layers of the atmosphere; (3) the higher nitrogen oxides emission from the automobiles, which would produce higher exhausts due to cold start in winter (Sun *et al.*, 2004). Little spatial variation was observed on sulfate and nitrate in spring and summer whereas relatively higher concentrations of the two ions were observed at HQ, HB and BC in winter and autumn.

Ammonium is primarily derived from the neutralization between atmospheric acidic species and ammonia vapor released from animal farming, fertilizers (in the form of ammonia/urea) and organic decomposition (Kumar and Sarin, 2010). The seasonal variation of ammonium was similar to that of sulfate and nitrate, with higher concentrations in winter and lower concentrations in other three seasons. Ammonium showed relatively even distribution at the 8 sites over Tianjin throughout the year.

Sea Salt

Despite the coastal location of the city, sea salt contributed only marginally (1.9–3.1%) to the PM_{10} mass at all sampling sites due to the northwesterly wind prevailing in Tianjin that blows from the inland receptor areas to the

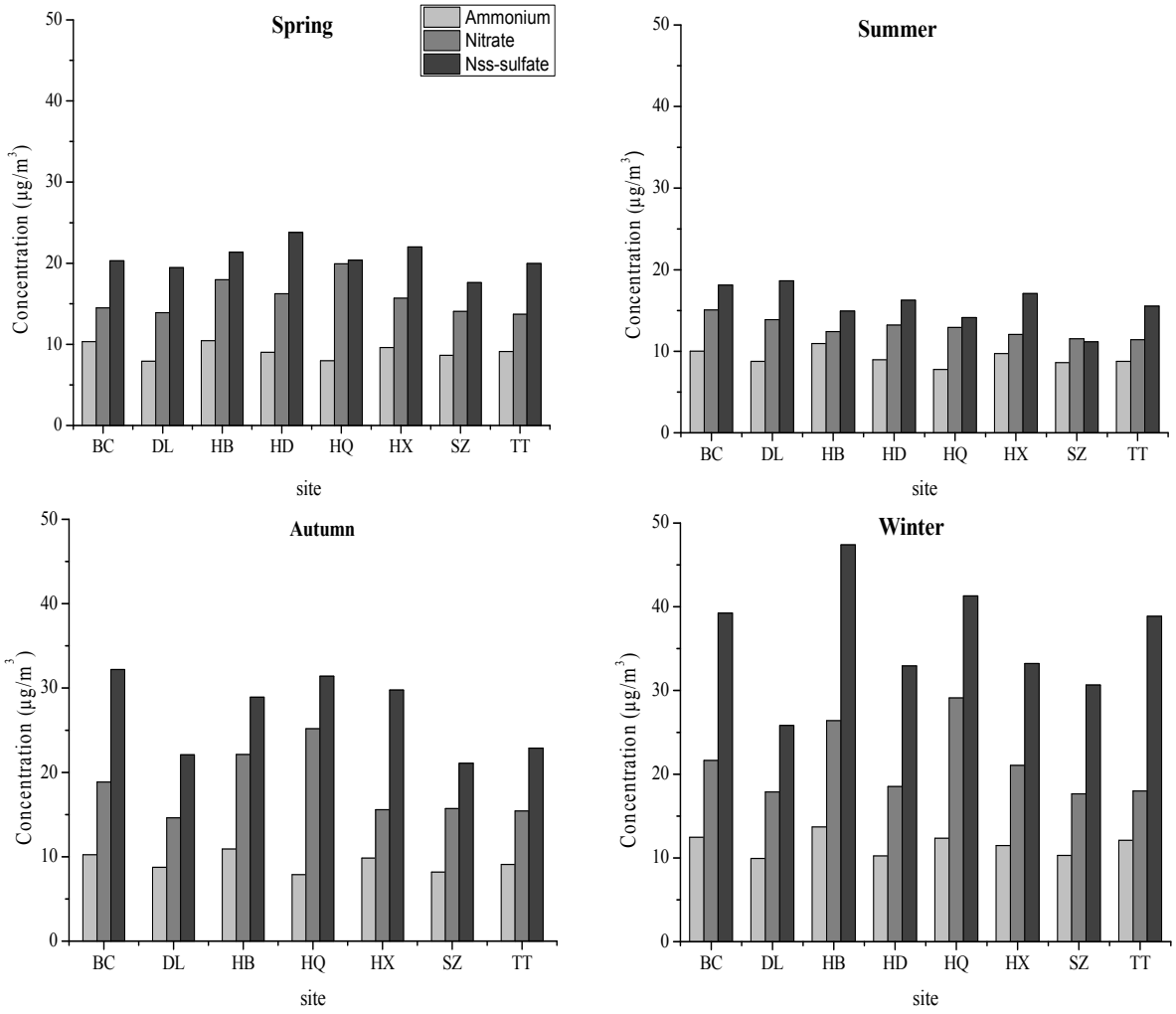

Fig. 4. Seasonal variation of ammonium, nitrate and non-sea salt sulfate concentrations (Nss-sulfate: non-sea salt sulfate)

coast. Similar contribution of sea salt was also found in Morogoro (Mkoma *et al.*, 2009) and Thessaloniki (Terzi *et al.*, 2010). Sea salt concentrations did not show significant ($P > 0.05$) spatial variation among the 8 sites (Fig. 2). The percentage contributions of sea salt during summer (3.4 ± 0.8%) were higher than those in spring (2.2 ± 0.3%), autumn (2.1 ± 0.4%) and winter (1.9 ± 0.5%) (Fig. 3). Concentrations of sea salt particles were generally higher in summer due to southeasterly winds prevailing during this season that transport air masses from the source areas along the coast to the inland receptor areas. Lower concentrations of sea salt were observed in spring, autumn and winter because of the change of prevailing wind direction in the three seasons in Tianjin.

Among the 8 sites, BC exhibited the highest concentrations of Ni, Cr, Mn, Zn, Sb, SO_4^{2-} and EC. And the concentrations of Ca, Ba, Pb and Sn at BC were aslo higher than at other sites (except for HQ). The high concentrations of EC, Ba, Zn, Pb, Sn and Sb at BC were due to its proximity to freeways with a large volume and high fraction of HDDVs while the high concentrations of Ca, Ni, Cr and Mn were attributed to the influence of industrial emissions such as cement production (Ca) and metallurgical processes (Ni, Cr and Mn). Among the 8 sites, HQ exhibited the highest concentrations of Si, Ca, Al, Fe, K, Mg, Ba, Pb, Sn, and the concentrations of Zn and Sb were also higher at HQ than at other sites (except for BC), due to emissions from the nearby construction sites and densely trafficked roads. HB exhibited high Ca concentration due to its proximity to construction sites. Both of HB and HQ showed high levels of SO_4^{2-} and NO_3^-. BC, HQ, DL and HB showed higher levels of organic matter compared with other four sites due to their proximity to the industrial zones with coal as the predominant fuels (BC and DL) or locations in the downwind of the industrial zones (HQ and HB). HX and SZ generally exhibited lower concentrations of chemical species than other sites, including Si, Al, Mg, K, Ca, Fe,V, Ni, Y, Mo, Ce and OC while TT and HD generally showed moderate concentrations of chemical species.

Fig. 5 shows a linear regression of the daily reconstructed and gravimetric mass concentrations for all 8 sites. Strong correlation was found between gravimetric and reconstructed mass, with a coefficient of determination (R^2) of 0.73, indicating overall good agreement between the reconstructed mass and the gravimetric mass. The seasonal trend in the correlation of the reconstructed and gravimetric mass

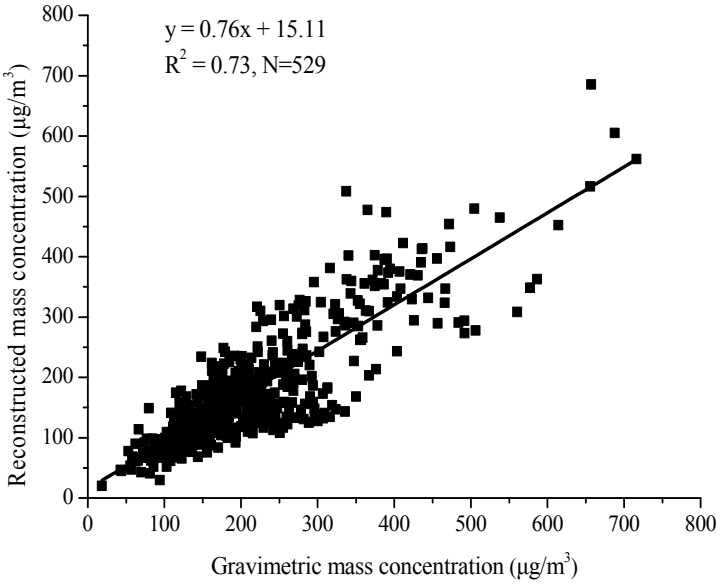

Fig. 5. Linear regression of reconstructed vs. gravimetric mass concentrations.

concentrations is demonstrated in Fig. 6. The season-based R^2 value ranged from 0.67 to 0.88. As in other studies (Putaud *et al.*, 2004; Rees *et al.*, 2004; Vecchi *et al.*, 2008; Vercauteren *et al.*, 2011), a total chemical mass closure of atmospheric PM was not achieved here, i.e., the overall identified aerosol components accounted for 82.5 ± 2.5% of the PM_{10} mass, with a seasonal variation of 86.0 ± 4.4%, 62.2 ± 1.8%, 89.3 ± 4.5%, 93.1 ± 5.0% for spring, summer, autumn and winter, respectively. The fractions of unidentified mass were considerably higher in summer than in other three seasons which coincide with other studies that showed higher unidentified mass fraction during summer than during winter (Cheung *et al.*, 2011). The unidentified fraction might be attributed to the water content of PM_{10}, the uncertainty in the OC multiplication factor and the inadequate estimation of crustal components. A study conducted in Switzerland investigated the water content of PM_{10}, and showed that it is higher in warmer (17.2%) season than in colder (6.0%) season (Hueglin *et al.*, 2005). Therefore the higher water content in summer may lead to the higher unidentified fraction. In this study, the factor of 1.6 was applied for all the 8 sites and over four seasons though the organic matter to OC ratio depends greatly on source characterization of organic component, which may induce some uncertainties in the overall estimations of organic matter to total mass. The organic matter might be underestimated, especially in summer, when biological materials play an important role for the organic matter (Plewka *et al.*, 2006) and the suggested conversion factor was around 2.2 for biological materials (Kunit and Puxbaum, 1996; Hueglin *et al.*, 2005). In addition, other possible reason for lack of closure could be artifacts during sampling and systematic errors in chemical analysis.

Correlations between PM_{10} Mass and Categories of Chemical Components

The Pearson correlation analysis was employed to determine the correlations between the concentrations of PM_{10} and the categories of chemical components. Crustal material concentration was found to correlate significantly ($P < 0.05$) with PM_{10} in spring (except for HX), autumn (except for HX) and winter (except for HX and HB), suggesting a major influence of crustal components on PM_{10}. Organic matter concentration had a significant ($P < 0.05$) correlation with PM_{10} in winter (except for HD), autumn, spring (except for HD and SZ) and summer (except for SZ and HQ), overall stressing the consistent nature of combustion source contributions in urban environment. The SIA concentration correlated significantly ($P < 0.05$) with the PM_{10} mass at all sites in four seasons, confirming the consistent contribution of SIA to PM_{10}. Trace elements concentration overall exhibited a significant ($P < 0.05$) correlation in four seasons while EC concentration had a significant ($P < 0.05$) correlation with PM_{10} only at some sites in autumn (DL, HQ and SZ) and summer (DL, HX and TT). It is interesting that the unidentified mass concentration correlated significantly ($P < 0.05$) with the PM_{10} mass at all sites in summer, which is difficult to explain. Unidentified mass concentration was also found to correlate highly with PM_{10} in Amsterdam (Sillanpaa *et al.*, 2006). In addition, sea salt concentration generally did not have a significant ($P > 0.05$) correlation with PM_{10} throughout the year in this study.

SUMMARYAND CONCLUSIONS

In this research, PM_{10} samples were collected every 6 days for one-year at 8 monitoring sites in Tianjin for the first time. The spatial and temporal variation of chemical composition and mass closure of PM_{10} were discussed in this paper. However, it should be noted that some limitations exist for the mass closure analysis. The water contents in PM_{10} samples were not determined in this study which may lead to the lack of closure, because the

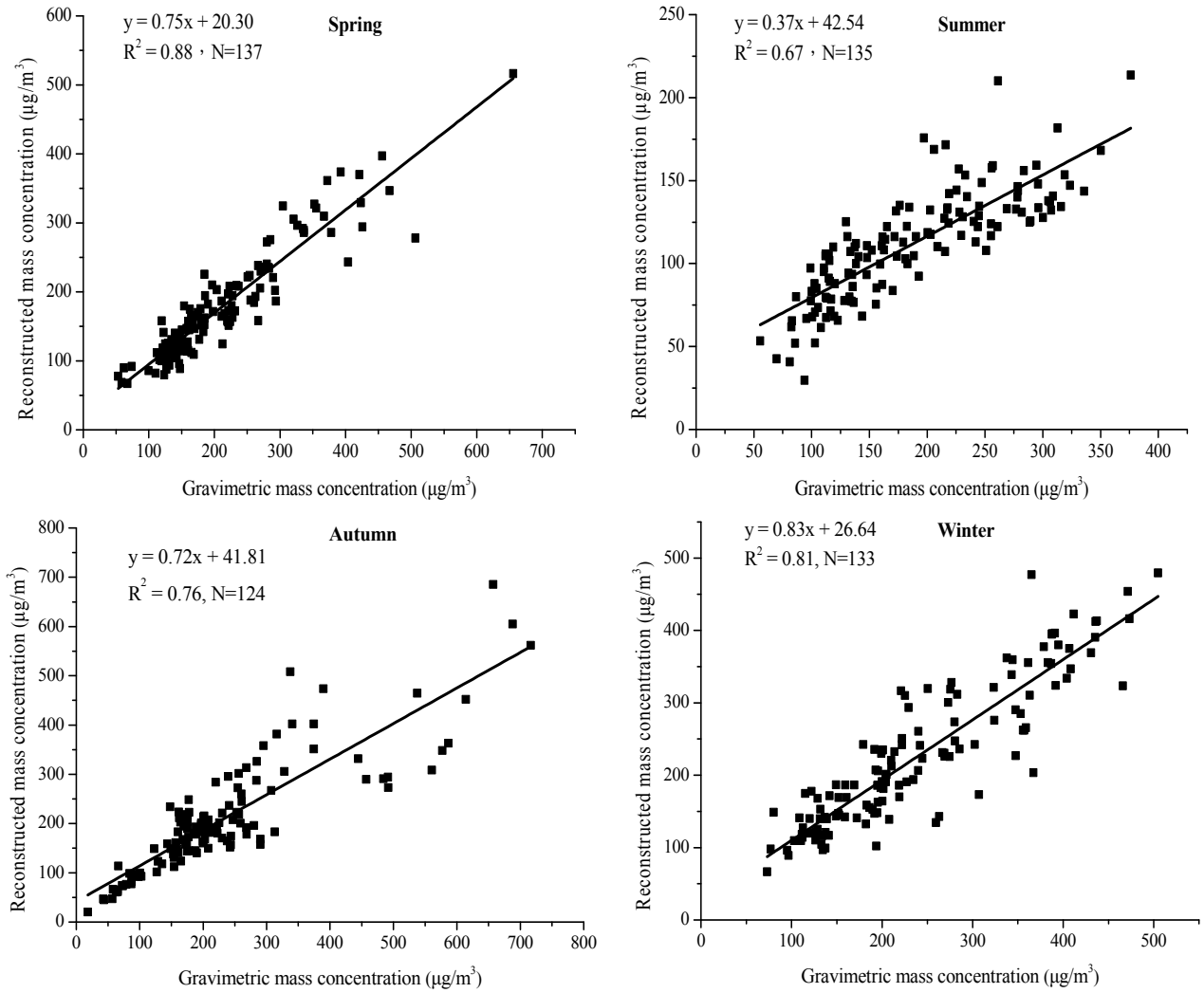

Fig. 6. Linear regression of reconstructed vs. gravimetric mass concentrations in four seasons.

hysteresis behaviour of aerosol particles can cause water to be retained on PM. Some uncertainties also exist in the multiplication factors for OM and crustal materials, which might induce the underestimation of these two compositions. In addition, the sampling sites did not cover rural sites where the characteristic of PM_{10} composition may be different from that in urban area. The sampling interval seems to be a little long, and sampling every 3 days could be better to reflect the variations of source emissions. Despite the limitations, the mass closure of PM_{10} at all 8 sites in Tianjin was done, which can reflect the differences in PM_{10} emission sources and processes, identify the major fractions and quantify their contributions to PM_{10}.

The major fractions of PM_{10} mass were crustal materials, organic matter, and secondary inorganic aerosol at all 8 sites in Tianjin. The chemical composition of PM_{10} exhibited significant spatial and seasonal variations. Crustal materials were the dominant fraction of PM_{10} with annual average percentages varying from 31.6% to 33.8% of the total PM_{10} mass. The concentrations and mass fractions of crustal materials were generally highest in spring and lowest in summer. Secondary inorganic aerosol (nss-sulfate, nitrate and ammonium) contributed on average 23.3% of the PM_{10} mass. In particular, nss-sulfate was the most predominant inorganic ion at all sites accounting for about 47.9% of the category of secondary inorganic aerosol, and 11.5% of total PM_{10} mass. The organic matter comprised a substantial portion of PM_{10}, with annual mass fraction of 18.8% while elemental carbon was a small category, accounting for 3.3%. The concentrations and relative contributions of organic matter and secondary inorganic aerosol in PM_{10} were generally highest in winter. Organic matter ($P < 0.05$) and EC ($P < 0.001$) concentrations showed significant spatial variations, and the concentrations were high at BC especially in winter due to its proximity to the industrial zones with coal as the predominant fuels and its location near freeways with higher number and proportion of heavy duty diesel vehicles. Sea salt and trace elements contributed marginally to the PM_{10} mass at all sites.

ACKNOWLEDGMENTS

The work presented in this paper was supported by the National Basic Research Program of China (2011CB503801).

REFERENCES

Bi, X., Feng, Y., Wu, J., Wang, Y. and Zhu, T. (2007). Source Apportionment of PM_{10} in Six Cities of Northern China. *Atmos. Environ.* 41: 903–912.

Cao, J.J., Wu, F., Chow, J.C., Lee, S.C., Li, Y., Chen, S.W., An, Z.S., Fung, K.K., Watson, J.G., Zhu, C.S. and Liu, S.X. (2005). Characterization and Source Apportionment of Atmospheric Organic and Elemental Carbon during Fall and Winter of 2003 in Xi'an, China. *Atmos. Chem. Phys.* 5: 3127–3137.

Cao, J.J., Lee, S.C., Chow, J.C., Watson, J.G., Ho, K.F., Zhang, R.J., Jin, Z.D., Shen, Z.X., Chen, G.C., Kang, Y.M., Zou, S.C., Zhang, L.Z., Qi, S.H., Dai, M.H., Cheng, Y. and Hu, K. (2007). Spatial and Seasonal Distributions of Carbonaceous Aerosols over China. *J. Geophys. Res.* 112: D22S11.

Chan, Y.C., Simpson, R.W., Mctainsh, G.H., Vowles, P.D., Cohen, D.D. and Bailey, G.M. (1999). Source Apportionment of $PM_{2.5}$ and PM_{10} Aerosols in Brisbane (Australia) by Receptor Modelling. *Atmos. Environ.* 33: 3251–3268.

Charron, A. and Harrison, R.M. (2005). Fine ($PM_{2.5}$) and Coarse ($PM_{2.5–10}$) Particulate Matter on a Heavily Trafficked London Highway: Sources and Processes. *Environ. Sci. Technol.* 39: 7768–7776.

Chester, R., Nimmo, M., Fones, G.R., Keyse, S. and Zhang, Z. (2000). Trace Metal Chemistry of Particulate Aerosols from the UK Mainland Coastal Rim of the NE Irish Sea. *Atmos. Environ.* 34: 949–958.

Cheung, K., Daher, N., Kam, W., Shafer, M.M., Ning, Z., Schauer, J.J. and Sioutas, C. (2011). Spatial and Temporal Variation of Chemical Composition and Mass Closure of Ambient Coarse Particulate Matter ($PM_{10–2.5}$) in the Los Angeles Area. *Atmos. Environ.* 45: 2651–2662.

China National Environmental Monitoring Centre. (1990). *The Elements Background Values in Chinese Soils*. Environmental Science Press of China, Beijing, p. 15–505 (in Chinese).

Clark, N.A., Demers, P.A., Karr, C.J., Koehoorn, M., Lencar, C., Tamburic, L. and Brauer, M. (2010). Effect of Early Life Exposure to Air Pollution on Development of Childhood Asthma. *Environ. Health Perspect.* 118: 284–290.

Du, X., Dong, S., Yang, F., Li, W., Wu, J. and Zhang, Q. (2010). *Tianjin Statistical Yearbook: Chapter 1: General Survey: Meteorological Data of Each Month, 2009,* China Statistics Press, Beijing.

Du, X., Dong, S., Yang, F., Wu, J., Zhang, Q. and Li, R. (2011). *Tianjin Statistical Yearbook: Chapter 1:General Survey: Meteorological Data of Each Month, 2010,* China Statistics Press, Beijing.

Gu, J., Bai, Z., Liu, A., Wu, L., Xie, Y., Li, W. Dong, H. and Zhang, X. (2010). Characterization of Atmospheric Organic Carbon and Element Carbon of $PM_{2.5}$ and PM_{10} at Tianjin, China. *Aerosol Air Qual. Res.* 10: 167–176.

Gugamsetty, B., Wei, H., Liu, C.N., Awasthi, A., Hsu, S.C., Tsai, C.J., Roam, G.D., Wu, Y.C. and Chen, C.F. (2012). Source Characterization and Apportionment of PM_{10}, $PM_{2.5}$ and $PM_{0.1}$ by Using Positive Matrix Factorization. *Aerosol Air Qual. Res.* 12: 476–491.

Han, B., Kong, S., Bai, Z., Du, G., Bi, T., Li, X., Shi, G. and Hu, Y. (2010). Characterization of Elemental Species in $PM_{2.5}$ Samples Collected in Four Cities of Northeast China. *Water Air Soil Pollut.* 209: 15–28.

Hart, J.E., Garshick, E., Dockery, D.W., Smith, T.J., Ryan, L. and Laden, F. (2011). Long-Term Ambient Multipollutant Exposures and Mortality. *Am. J. Respir. Crit. Care Med.* 183: 73–78.

Hjortenkrans, D.S.T., Bergback, B.G. and Haggerud, A.V. (2007). Metal Emissions from Brake Linings and Tires: Case Studies of Stockholm, Sweden 1995/1998 and 2005. *Environ. Sci. Technol.* 41: 5224–5230.

Ho, K.F., Lee, S.C., Cao, J.J., Chow, J.C., Watson, J.G. and Chan, C.K. (2006). Seasonal Variations and Mass Closure Analysis of Particulate Matter in Hong Kong. *Sci. Total Environ.* 355: 276–287.

Hueglin, C., Gehrig, R., Baltensperger, U., Gysel, M., Monn, C. and Vonmont, H. (2005). Chemical Characterisation of $PM_{2.5}$, PM_{10} and Coarse Particles at urban, near-city and Rural Sites in Switzerland. *Atmos. Environ.* 39: 637–651.

IPCC (2001). In *Climate Change 2001: The Scientific Basis.Contributio n of Working Group I to the Third Assessment Report of the Intergovernmental Panel on Climate Change,* Houghton, J.T., Ding, Y., Griggs, D.J., Noguer, M., van der Linden, P.J., Dai, X., Maskell, K. and Johnson, C.A. (Eds.), Cambridge University Press, Cambridge, UK, New York, NY, USA. p. 881.

Khoder, M.I. (2002). Atmospheric Conversion of Sulfur Dioxide to Particulate Sulfate and Nitrogen Dioxide to Particulate Nitrate and Gaseous Nitric Acid in an Urban Area. *Chemosphere* 49: 675–684.

Kim, K.H., Choi, B.J., Yun, S.T. and Hwang, S.J. (2004). Studies of Spatial and Temporal Distribution Characteristics of TSP-bound Trace Metals in Seoul, Korea. *Environ. Pollut.*127: 323–333.

Kleeman, M.J., Riddle, S.G., Robert, M.A. and Jakober, C.A. (2008). Lubricating Oil and Fuel Contributions to Particulate Matter Emissions from Light-duty Gasoline and Heavy-duty Diesel Vehicles. *Environ. Sci. Technol.* 42: 235–242.

Kong, S., Han, B., Bai, Z., Chen, L., Shi, J. and Xu, Z. (2010). Receptor modeling of $PM_{2.5}$, PM_{10} and TSP in Different Seasons and Long-range Transport Analysis at a Coastal site of Tianjin, China. *Sci. Total Environ.* 408: 4681–4694.

Kong, S., Ji, Y., Lu, B., Chen, L., Han, B., Li, Z. and Bai, Z. (2011a). Characterization of PM_{10} Source Profiles for Fugitive Dust in Fushun-A City Famous for Coal. *Atmos. Environ.* 45: 5351–5365.

Kong, S., Lu, B., Bai, Z., Zhao, X., Chen, L., Han, B., Li, Z., Ji, Y., Xu, Y., Liu, Y. and Jiang, H. (2011b). Potential Threat of Heavy Metals in Re-suspended Dusts on Building Surfaces in Oilfield City. *Atmos. Environ.* 45: 4192–4204.

Kumar, A. and Sarin, M.M. (2010). Atmospheric Water-soluble Constituents in Fine and Coarse Mode Aerosols from High-altitude Site in Western India: Long-range

Transport and Seasonal Variability. *Atmos. Environ.* 44: 1245–1254.

Kunit, M. and Puxbaum, H. (1996). Enzymatic Determination of the Cellulose Content of Atmospheric Aerosols. *Atmos. Environ.* 30: 1233–1236.

Lazaridis, M., Semb, A., Larssen, S., Hjellbrekke, A.G., Hov, O., Hanssen, J.E., Schaug, J. and Torseth, K. (2002). Measurements of Particulate Matter within the Framework of the European Monitoring and Evaluation Programme (EMEP) I. First Results. *Sci. Total Environ.* 285: 209–235.

Li, M., Huang, X., Zhu, L., Li, J., Song, Y., Cai, X. and Xie, S. (2012). Analysis of the Transport Pathways and Potential Sources of PM_{10} in Shanghai Based on Three Methods. *Sci. Total Environ.* 414: 525–534.

Louie, P., Watson, J., Chow, J., Chen, A., Sin, D. and Lau, A. (2005). Seasonal Characteristics and Regional Transport of $PM_{2.5}$ in Hong Kong. *Atmos. Environ.* 39: 1695–1710.

Marcazzan, G.M., Vaccaro, S., Valli, G. and Vecchi, R. (2001). Characterisation of PM_{10} and $PM_{2.5}$ Particulate Matter in the Ambient Air of Milan (Italy). *Atmos. Environ.* 35: 4639–4650.

Matta, E., Facchini, M.C., Decesari, S., Mircea, M., Cavalli, F., Fuzzi, S., Putaud, J.P. and Dell'Acqua, A. (2003). Mass closure on the chemical species in size-Segregated Atmospheric Aerosol Collected in an Urban Area of the Po Valley, Italy. *Atmos. Chem. Phys.* 3: 623–637.

Ministry of Environmental Protection of the People's Republic of China (1996). *National Ambient Air Quality Standard*, http://www.nthb.cn/standard/standard03/20030411161748.html.

Ministry of Environmental Protection of the People's Republic of China (2012). *National Ambient Air Quality Standard*, http://kjs.mep.gov.cn/hjbhbz/bzwb/dqhjbh/dqhjzlbz/201203/t20120302_20224165.htm.

Mkoma, S.L., Maenhaut, W., Chi, X., Wang, W. and Raes, N. (2009). Characterisation of PM_{10} Atmospheric Aerosols for the Wet Season 2005 at Two Sites in East Africa. *Atmos. Environ.* 43: 631–639.

Ni, T., Han, B. and Bai, Z. (2012). Source Apportionment of PM_{10} in Four Cities of Northeastern China. *Aerosol Air Qual. Res.* 12: 571–582.

Oanh, N.T.K., Thiansathit, W., Bond, T.C., Subramanian, R., Winijkul, E. and Paw-armart, I. (2010). Compositional Characterization of $PM_{2.5}$ Emitted from in-use Diesel Vehicles. *Atmos. Environ.* 44: 15–22.

Ohlson, C.G., Berg, P., Bryngelsson, I.L., Elihn, K., Ngo, Y., Westberg, H. and Sjogren, B. (2010). Inflammatory Markers and Exposure to Occupational Air Pollutants. *Inhalation Toxicol.* 22: 1083–1090.

Perrino, C., Canepari, S., Pappalardo, S. and Marconi, E. (2010). Time-resolved Measurements of Water-soluble Ions and Elements in Atmospheric Particulate Matter for the Characterization of Local and Long-range Transport Events. *Chemosphere* 80: 1291–1300.

Plewka, A., Gnauk, T., Brueggemann, E. and Herrmann, H. (2006). Biogenic Contributions to the Chemical Composition of Airborne Particles in a Coniferous Forest in Germany. *Atmos. Environ.* 40: S103–S115.

Putaud, J.P., Raes, F., Van Dingenen, R., Bruggemann, E., Facchini, M.C., Decesari, S., Fuzzi, S., Gehrig, R., Huglin, C., Laj, P., Lorbeer, G., Maenhaut, W., Mihalopoulos, N., Mulller, K., Querol, X., Rodriguez, S., Schneider, J., Spindler, G., ten Brink, H., Torseth, K. and Wiedensohler, A. (2004). European Aerosol Phenomenology-2: Chemical Characteristics of Particulate Matter at kerbside, Urban, Rural and Background Sites in Europe. *Atmos. Environ.* 38: 2579–2595.

Rees, S.L., Robinson, A.L., Khlystov, A., Stanier, C.O. and Pandis, S.N. (2004). Mass Balance Closure and the Federal Reference Method for $PM_{2.5}$ in Pittsburgh, Pennsylvania. *Atmos. Environ.* 38: 3305–3318.

Saitanis, C.J., Frontasyeva, M.V., Steinnes, E., Palmer, M.W., Ostrovnaya, T.M. and Gundorina, S.F. (2013). Spatiotemporal Distribution of Airborne Elements Monitored with the Moss Bags Technique in the Greater Thriasion Plain, Attica, Greece. *Environ. Monit. Assess.* 185: 955–968.

Sandstrom, T., Cassee, F.R., Salonen, R. and Dybing, E. (2005). Recent Outcomes in European Multicentre Projects on Ambient Particulate Air Pollution. *Toxicol. Appl. Pharmacol.* 207: 261–268.

Sanhueza, P.A., Torreblanca, M.A., Diaz-Robles, L.A., Schiappacasse, L.N., Silva, M.P. and Astelle, T.D. (2009). Particulate Air Pollution and Health Effects for Cardiovascular and Respiratory Causes in Temuco, Chile: A Wood-Smoke-Polluted Urban Area. *J. Air Waste Manage. Assoc.* 59: 1481–1488.

Seinfeld, J.H. and Pandis, S.N. (2006). *Atmospheric Chemistry and Physics- From Pollution to Climate Change,* John Wiley & Sons, Inc, New York.

Sillanpaa, M., Hillamo, R., Saarikoski, S., Frey, A., Pennanen, A., Makkonen, U., Spolnik, Z., Van Grieken, R., Branis, M., Brunekreef, B., Chalbot, M.C., Kuhlbusch, T., Sunyer, J., Kerminen, V.M., Kulmala, M. and Salonen, R.O. (2006). Chemical Composition and Mass Closure of Particulate Matter at Six Urban Sites in Europe. *Atmos. Environ.* 40: S212–S223.

Singh, K., Singh, D.P., Dixit, C.K., Singh, N., Sharma, C., Sahai, S., Jha, A.K., Khan, Z.H. and Gupta, P.K. (2012). Chemical Characteristics of Aerosols and Trace Gas Distribution over North and Central India. *Environ. Monit. Assess.* 184: 4553–4564.

Stelson, W.T. and Seinfeld, J.H. (1982). Relative Humidity and Temperature Dependence of the Ammonium Nitrate Dissociation Constant. *Atmos. Environ.* 16: 983–992.

Sun, Y., Pan, Y.P., Li, X.R., Zhu, R.H. and Wang, Y.S. (2011). Chemical Composition and Mass Closure of Particulate Matter in Beijing, Tianjin and Hebei Megacities, Northern China. *Huanjing Kexue.* 32: 2732–2740 (in Chinese).

Sun, Y.L., Zhuang, G.S., Ying, W., Han, L.H., Guo, J.H., Mo, D., Zhang, W.J., Wang, Z.F. and Hao, Z.P. (2004). The Air-borne Particulate Pollution in Beijing - Concentration, Composition, Distribution and Sources. *Atmos. Environ.* 38: 5991–6004.

Tecer, L.H., Tuncel, G., Karaca, F., Alagha, O., Suren, P., Zararsiz, A. and Kirmaz, R. (2012). Metallic Composition

and Source Apportionment of Fine and Coarse Particles Using Positive Matrix Factorization in the Southern Black Sea Atmosphere. *Atmos. Res.* 118: 153–169.

Terzi, E., Argyropoulos, G., Bougatioti, A., Mihalopoulos, N., Nikolaou, K. and Samara, C. (2010). Chemical Composition and Mass Closure of Ambient PM_{10} at Urban Sites. *Atmos. Environ.* 44: 2231–2239.

Tsai, Y.I. and Chen, C.L. (2006). Atmospheric Aerosol Composition and Source Apportionments to Aerosol in Southern Taiwan. *Atmos. Environ.* 40: 4751–4763.

Turpin, B.J. and Lim, H.J. (2001). Species Contributions to $PM_{2.5}$ Mass Concentrations: Revisiting Common Assumptions for Estimating Organic Mass. *Aerosol Sci. Technol.* 35: 602–610.

Vecchi, R., Chiari, M., D'Alessandro, A., Fermo, P., Lucarelli, F., Mazzei, F., Nava, S., Piazzalunga, A., Prati, P., Silvani, F. and Valli, G. (2008). A Mass Closure and PMF Source Apportionment Study on the Sub-micron Sized Aerosol Fraction at Urban Sites in Italy. *Atmos. Environ.* 42: 2240–2253.

Vercauteren, J., Matheeussen, C., Wauters, E., Roekens, E., van Grieken, R., Krata, A., Makarovska, Y., Maenhaut, W., Chi, X. and Geypens, B. (2011). Chemkar PM_{10}: An Extensive Look at the Local Differences in Chemical Composition of PM_{10} in Flanders, Belgium. *Atmos. Environ.* 45: 108–116.

Viana, M., Maenhaut, W., Chi, X., Querol, X. and Alastuey, A. (2007). Comparative Chemical Mass Closure of Fine and Coarse Aerosols at Two Sites in South and West Europe: Implications for EU Air Pollution Policies. *Atmos. Environ.* 41: 315–326.

Wang, S.W., Zhang, Q., Streets, D.G., He, K.B., Martin, R.V., Lamsal, L.N., Chen, D., Lei, Y. and Lu, Z. (2012). Growth in NO_x Emissions from Power Plants in China: Bottom-up Estimates and Satellite Observations. *Atmos. Chem. Phys.* 12: 4429–4447.

Wang, X., Bi, X., Sheng, G. and Fu, J. (2006a). Chemical Composition and Sources of PM_{10} and $PM_{2.5}$ Aerosols in Guangzhou, China. *Environ. Monit. Assess.* 119: 425–439.

Wang, Y., Zhuang, G.S., Zhang, X.Y., Huang, K., Xu, C., Tang, A.H., Chen, J.M. and An, Z.S. (2006b). The Ion Chemistry, Seasonal Cycle, and Sources of $PM_{2.5}$ and TSP Aerosol in Shanghai. *Atmos. Environ.* 40: 2935–2952.

Watson, J.G. (2002). Visibility: Science and Regulation. *J. Air Waste Manage. Assoc.* 52: 628–713.

Wei, F., Teng, E., Wu, G., Hu, W., Wilson, W.E., Chapman, R.S., Pau, J.C. and Zhang, J. (1999). Ambient Concentrations and Elemental Compositions of PM_{10} and $PM_{2.5}$ in Four Chinese Cities. *Environ. Sci. Technol.* 33: 4188–4193.

Wu, Y., Ji, D.S., Song, T., Zhu, B. and Wang, Y.S. (2011). Characteristics of Atmospheric Pollutants in Beijing, Zhuozhou, Baoding and Shijiazhuang During the Period of Summer and Autumn. *Huanjing Kexue*. 32: 2741–2749.

Xiu, G.L., Zhang, D.N., Chen, J.Z., Huang, X.J., Chen, Z.X., Guo, H.L. and Pan, J.F. (2004). Characterization of Major Water-soluble Inorganic Ions in Size-fractionated Particulate Matters in Shanghai Campus Ambient Air. *Atmos. Environ.* 38: 227–236.

Yu, I.T.S., Zhang, Y.H., Tam, W.W.S., Yan, Q.H., Xu, Y.J., Xun, X.J., Wu, W., Ma, W.J., Tian, L.W., Tse, L.A. and Qian, X. (2012). Effect of Ambient Air Pollution on Daily Mortality Rates in Guangzhou, China. *Atmos. Environ.* 46: 528–535.

Zhang, Q., Streets, D.G., He, K., Wang, Y., Richter, A., Burrows, J.P., Uno, I., Jang, C.J., Chen, D., Yao, Z. and Lei, Y. (2007). NO_x Emission Trends for China, 1995–2004: The View from the Ground and the View from Space. *J. Geophys. Res.* 112: D22306.

Zhang, R., Ho, K.F., Cao, J., Han, Z., Zhang, M., Cheng, Y. and Lee, S.C. (2009). Organic Carbon and Elemental Carbon Associated with PM_{10} in Beijing during Spring Time. *J. Hazard. Mater.* 172: 970–977.

Received for review, October 12, 2012
Accepted, March 9, 2013